

## Studying periodic nanostructures by probing the in-sample optical far-field using coherent phonons

C. Brüggemann, J. Jäger, B. A. Glavin, V. I. Belotelov, I. A. Akimov et al.

Citation: *Appl. Phys. Lett.* **101**, 243117 (2012); doi: 10.1063/1.4771986

View online: <http://dx.doi.org/10.1063/1.4771986>

View Table of Contents: <http://apl.aip.org/resource/1/APPLAB/v101/i24>

Published by the [American Institute of Physics](#).

### Related Articles

Negative Gaussian curvature distribution in physical and biophysical systems—Curved nanocarbons and ion-channel membrane proteins

*J. Appl. Phys.* **112**, 114316 (2012)

Room-temperature ferromagnetism in Co-doped CeO<sub>2</sub> nanospheres prepared by the polyvinylpyrrolidone-assisted hydrothermal method

*J. Appl. Phys.* **112**, 113904 (2012)

Surface-enhanced Raman scattering (SERS) based on copper vanadate nanoribbon substrate: A direct bio-detection without surface functionalization

*J. Appl. Phys.* **112**, 114309 (2012)

Modeling plasmonics: A Huygens subgridding scheme for Lorentz media

*J. Chem. Phys.* **137**, 204111 (2012)

Structural study of Bi<sub>2</sub>Sr<sub>2</sub>CaCu<sub>2</sub>O<sub>8+δ</sub> exfoliated nanocrystals

*Appl. Phys. Lett.* **101**, 223106 (2012)

### Additional information on *Appl. Phys. Lett.*

Journal Homepage: <http://apl.aip.org/>

Journal Information: [http://apl.aip.org/about/about\\_the\\_journal](http://apl.aip.org/about/about_the_journal)

Top downloads: [http://apl.aip.org/features/most\\_downloaded](http://apl.aip.org/features/most_downloaded)

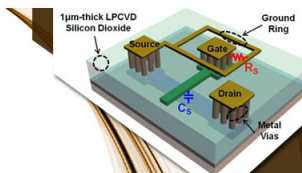
Information for Authors: <http://apl.aip.org/authors>

## ADVERTISEMENT



**EXPLORE WHAT'S  
NEW IN APL**

**SUBMIT YOUR PAPER NOW!**



### **SURFACES AND INTERFACES**

Focusing on physical, chemical, biological, structural, optical, magnetic and electrical properties of surfaces and interfaces, and more...



### **ENERGY CONVERSION AND STORAGE**

Focusing on all aspects of static and dynamic energy conversion, energy storage, photovoltaics, solar fuels, batteries, capacitors, thermoelectrics, and more...

# Studying periodic nanostructures by probing the in-sample optical far-field using coherent phonons

C. Brüggemann,<sup>1,a)</sup> J. Jäger,<sup>1</sup> B. A. Glavin,<sup>2</sup> V. I. Belotelov,<sup>3</sup> I. A. Akimov,<sup>1,4</sup> S. Kasture,<sup>5</sup> A. V. Gopal,<sup>5</sup> A. S. Vengurlekar,<sup>5</sup> D. R. Yakovlev,<sup>1,4</sup> A. V. Akimov,<sup>4,6</sup> and M. Bayer<sup>1,4</sup>

<sup>1</sup>Experimentelle Physik 2, Technische Universität Dortmund, 44221 Dortmund, Germany

<sup>2</sup>Lashkaryov Institute of Semiconductor Physics, 03028 Kyiv, Ukraine

<sup>3</sup>Lomonosov Moscow State University, 119991 Moscow, Russia

<sup>4</sup>Ioffe Physical-Technical Institute, Russian Academy of Sciences, 194021 St. Petersburg, Russia

<sup>5</sup>Tata Institute of Fundamental Research, 400005 Mumbai, India

<sup>6</sup>School of Physics and Astronomy, University of Nottingham, Nottingham NG7 2RD, United Kingdom

(Received 30 October 2012; accepted 26 November 2012; published online 13 December 2012)

Optical femtosecond laser pulses diffracted into a crystalline substrate by a gold grating on top interact with gigahertz coherent phonons propagating towards the grating from the opposite side. As a result, Brillouin oscillations are detected for diffracted light. The experiment and theoretical analysis show that the amplitude of the oscillations for the first order diffracted light exceeds that of the zero order signal by more than ten times. The results provide a method for internal probing of the optical far-field inside materials containing periodic nanostructures. © 2012 American Institute of Physics. [<http://dx.doi.org/10.1063/1.4771986>]

Coherent acoustic phonons in the gigahertz (GHz) and terahertz (THz) frequency range have been widely used for probing optical properties of solids. Most established is the picosecond acoustic interferometry in optically transparent materials.<sup>1,2</sup> The underlying physics of this method is sketched in Fig. 1(a). A broad spectrum wavepacket of coherent phonons (e.g., a picosecond strain pulse) propagating with the sound velocity  $s$  towards the sample surface modulates the dielectric permittivity  $\epsilon$  of the solid. This dynamical modulation results in a partial reflection of an incident optical pulse by the coherent phonons (in analogy to Brillouin scattering in non-coherent acoustics). When the reflected light pulse leaves the sample, it interferes with the optical pulse that has been reflected at the sample surface under the specular angle  $\alpha$ . The intensity of the resulting reflected beam shows oscillations as a function of the temporal separation  $t$  between the optical pulse and the acoustic coherent phonon wavepacket. The radial frequency of these oscillations, often called Brillouin frequency, is equal to

$$\omega_0 = 4\pi s \sqrt{\epsilon - \sin^2 \alpha} / \lambda, \quad (1)$$

where  $\lambda$  is the center wavelength of the optical pulse in vacuum. The measurement of  $\omega_0$  has been widely used during the last 20 years to study optical, elastic, and elasto-optical properties in crystalline and amorphous bulk materials and thin films.<sup>1–8</sup>

Recently, GHz and THz phonons have been employed to study periodic optical nanostructures like photonic, plasmonic, and phononic crystals which are attractive for various applications. Most of these works with coherent phonons targeted specific properties of the nanostructures by probing the electromagnetic field inside the studied nanostructure. Thus, the interaction of the vibrational phonon modes and light was studied experimentally by picosecond acoustic techniques in

periodic structures which possess both photonic and phononic band gaps (i.e., photonic-phononic crystals),<sup>9,10</sup> hole arrays,<sup>11</sup> metallic gratings,<sup>12–14</sup> and complex periodic plasmonic nanostructures.<sup>15</sup> Less attention was paid to the elasto-optical effects that occur in bulk solid media at a distance from the nanostructure larger than the optical wavelength, where light has a well-defined wavevector and a corresponding propagation direction.<sup>16</sup> The spatial and spectral distributions of this far-field region are changed due to

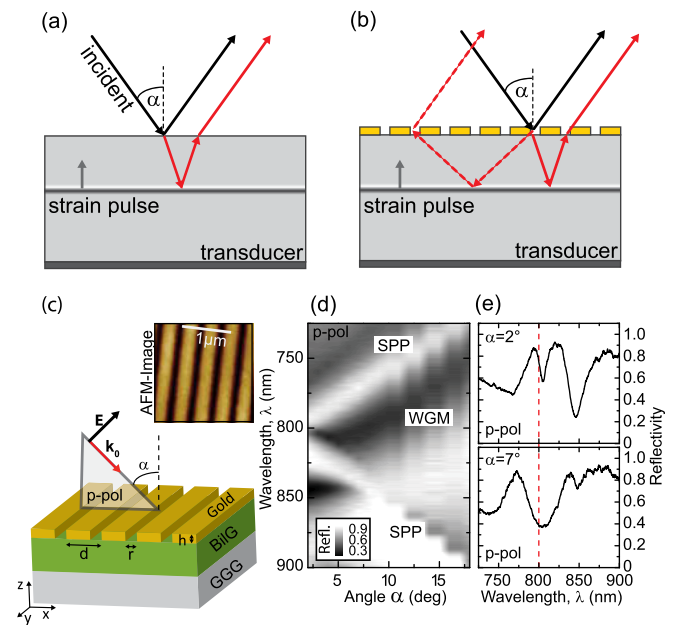


FIG. 1. Schemes of picosecond acoustic interferometry in optically transparent materials for a plain surface (a) and a periodic planar nanostructure (b). (c) Atomic microscope image of the studied sample and experimental setup. (d) Contour plot of angle dependent reflectivity, measured with a white light source: surface plasmon-polariton (SPP) resonances and waveguiding mode (WGM) are observed. (e) Reflectivity spectra measured at incidence angles  $\alpha = 2^\circ$  and  $\alpha = 7^\circ$ ; the vertical dashed line shows the wavelength,  $\lambda = 800$  nm, of the optical probe pulse.

<sup>a)</sup>Email: christian.brueggemann@tu-dortmund.de.

the diffraction of light by a periodic nanostructure. Consequently, its interaction with coherent phonons becomes more complex than in case of a plain homogeneous surface, shown in Fig. 1(a), possibly opening new perspectives.

Figure 1(b) shows a sketch of a picosecond acoustic interferometry experiment involving light incident on a diffraction grating. The diffracted light propagating in the solid interacts with the coherent phonons similar to the simple case illustrated in Fig. 1(a), but the propagation direction of the diffracted beam, shown by dashed red lines in Fig. 1(b), is different. Therefore, the Brillouin oscillation frequency of the reflected light will be different from the one given by Eq. (1). For instance, for the first negative order of diffraction it is easy to show that

$$\omega_{-1} = 4\pi s \sqrt{\epsilon - (\lambda/d - \sin \alpha)^2} / \lambda, \quad (2)$$

where  $d$  is the grating period. More complex are the amplitudes of the acoustic interferometry signals for different diffraction orders. They depend on the intensity of the diffracted beams, the spectrum of the coherent phonon wavepacket, and the elasto-optical interaction between the coherent phonons and the electromagnetic wave.

In the present work, we address the interaction of optical pulses with coherent phonons in the far-field region of a short-period diffraction grating inside a sample on top of which the grating is placed. We show experimentally that using picosecond acoustic interferometry results in strong optical signals which oscillate with a frequency characteristic for the diffracted beam. A comprehensive theoretical analysis confirms the experimental observations and provides a strategy for designing nanostructures, where the interaction of light with coherent phonons can be deliberately exploited, e.g., for high-frequency acoustic nanoscopy.<sup>17</sup>

The experimental scheme and the atomic force microscope image of the sample surface are shown in Fig. 1(c). The periodic nanostructure was a gold (Au) grating fabricated on top of the (111) plane of a 0.5 mm thick gadolinium gallium garnet  $\text{Gd}_3\text{Ga}_5\text{O}_{12}$  (GGG) substrate with an intermediate bismuth-substituted rare-earth iron garnet (BiIG) film.<sup>18,19</sup> The grating period  $d = 400$  nm, thickness of the Au stripes  $h = 80$  nm, as well as the width of the slits  $r = 115$  nm and the BiIG layer thickness (355 nm) were optimized to have distinct spectral dips over a wide spectral range in the optical reflectivity spectra. Exemplary spectra are shown in Fig. 1(d) for  $\lambda = 700 - 1000$  nm and incidence angles  $\alpha = 2^\circ - 18^\circ$ , and the ones for  $\alpha = 2^\circ$  and  $7^\circ$  are highlighted in Fig. 1(e). The spectra for  $p$ -polarized light (electric field perpendicular to the grating stripes) consist of Wood anomalies which are governed by plasmon-polariton resonances in the Au grating and a waveguiding mode in the BiIG film.<sup>18,19</sup> The waveguiding mode is also present for  $s$ -polarization (not shown here).

In our picosecond acoustic interferometry experiments, carried out at room temperature, the coherent phonons were generated at the sample side opposite to the grating by illuminating a 50 nm thick Al film by optical pump pulses from a femtosecond laser with a regenerative amplifier (pulse duration 150 fs, repetition rate 100 kHz,  $\lambda = 800$  nm, excitation

spot with 100  $\mu\text{m}$  diameter, maximum excitation density  $W \sim 10$  mJ/cm<sup>2</sup> at the surface). Optical excitation of the Al film results in the injection of a bipolar strain pulse into the GGG substrate with an amplitude up to  $10^{-3}$  and  $\sim 10$  ps duration.<sup>20</sup> Such a strain pulse corresponds to a wavepacket of coherent longitudinal acoustic phonons covering a wide spectrum centered around 50 GHz. The coherent phonons propagate through the GGG substrate and after a time of  $\sim 80$  ns, they hit the Au grating. They are monitored by measuring the intensity change  $\Delta I(t)$  of optical probe pulses, originating from the same femtosecond laser, that have been reflected from the grating. Temporal resolution is achieved by variation of the delay  $t$  between the probe pulse and strain pulse excitation (pump).

Probe signals  $\Delta I_{s,p}(t)$  measured for  $\alpha = 7^\circ$  are shown in Fig. 2(a). The lower case index in  $\Delta I_{s,p}(t)$  corresponds to the polarization ( $s$  or  $p$ ) of the incident probe beam. The upper and middle curves correspond to  $\Delta I_s(t)$  and  $\Delta I_p(t)$ , respectively. Both signals show oscillations which start earlier for  $\Delta I_p(t)$  than for  $\Delta I_s(t)$ . For  $s$ -polarization, a non-zero value of  $\Delta I_s$  is detected only at  $t > 0$ , where we assign  $t = 0$  to the temporal moment when the acoustic wave packet hits the Au grating. The origin of the signals  $\Delta I_{s,p}(t)$  measured for  $t > 0$  was described in earlier works with metallic gratings and corresponds mainly to the acoustic modulation of the electromagnetic near-field by coherent phonons.<sup>11-14</sup> The signal  $\Delta I_p(t)$  measured with  $p$ -polarized light shows oscillatory behavior for  $t < 0$  starting already at  $t > -400$  ps when the coherent phonons are propagating mostly in GGG. They reach the BiIG layer at  $t \approx -50$  ps and subsequently at  $t = 0$  hit the Au grating. The observation of the oscillations in

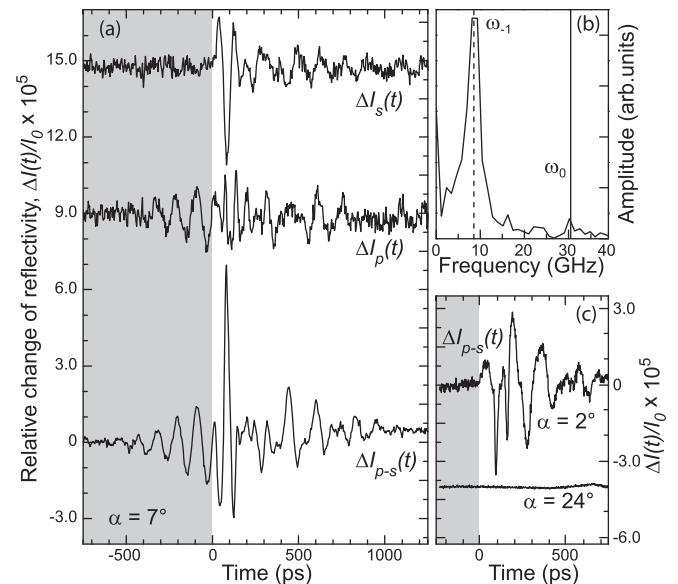


FIG. 2. (a) Temporal evolutions of the probe signals  $\Delta I_s(t)$  and  $\Delta I_p(t)$ , measured for  $s$ - and  $p$ -probe light polarizations, respectively, and  $\Delta I_{p-s}(t)$  measured with a balanced detection scheme at an incidence angle  $\alpha = 7^\circ$ ; the shaded area corresponds to the temporal interval when Brillouin oscillations are detected due to internal far-field probing. (b) Fast Fourier transform obtained from  $\Delta I_{p-s}(t)$ ; the solid and dashed vertical lines indicate the calculated frequency for the oscillations corresponding to non-diffracted and diffracted light, respectively. (c)  $\Delta I_{p-s}(t)$  measured for  $\alpha = 2^\circ$  and  $\alpha = 24^\circ$ , where the far-field signals at  $t < 0$  are not observed. Zero levels in (a) and (c) are shifted for clarity.

$\Delta I_p(t)$  at  $t < 0$  is the main experimental result of interest here. The bottom curve in Fig. 2(a) shows the signal measured at  $\alpha = 7^\circ$  using a balanced detection scheme. In this case, the incident beam has  $s$ - and  $p$ -polarization components of equal intensity and the balanced detector measures the difference of reflectivity for  $s$ - and  $p$ -polarized light. The balanced signal  $\Delta I_{p-s}(t)$  contains much less noise compared to  $\Delta I_{s,p}(t)$ . At  $t < 0$ ,  $\Delta I_{p-s}(t) = \Delta I_p(t)$ , because then  $\Delta I_s(t) = 0$  [see upper curve in Fig. 2(a)]. Figure 2(b) shows the fast Fourier transform (FFT) of the measured signal  $\Delta I_{p-s}(t)$  determined for the time interval from  $t = -850$  ps to  $t = 0$ . The FFT shows a spectral line centered at  $f = 8.5$  GHz with a width of  $\Delta f = 2.5$  GHz. Figure 2(c) shows  $\Delta I_{p-s}(t)$  measured for  $\alpha = 2^\circ$  and  $\alpha = 24^\circ$ . For  $\alpha = 2^\circ$   $\Delta I_{p-s}(t)$  is non-zero only for  $t > 0$ , while  $\Delta I_{p-s}(t)$  is negligible at any  $t$  for  $\alpha = 24^\circ$ .

The main goal of our analysis is to understand the origin of the signal  $\Delta I_{p-s}(t)$  at  $t < 0$ , where the acoustic phonon wavepacket did not yet hit the Au grating. The natural approach to understand the experimental result is to seek for an explanation based on the picosecond acoustic interferometry schemes in Figs. 1(a) and 1(b). The measured value of the oscillation frequency, 8.5 GHz, is much smaller than the one calculated using Eq. (1), which amounts to 31 GHz ( $s = 6400$  m/s (Ref. 21) and  $\epsilon = 3.8$  (Ref. 22) for GGG). However, it is close to the value obtained from Eq. (2), which yields an oscillation frequency of 8.3 GHz. This corresponds to the case in which the measured signal is related to

the beam that has been diffracted into the GGG substrate by the Au grating. Thus, we may explain the oscillations detected for  $t < 0$  by interference of the two parts of the probe beam as shown in Fig. 1(b): one is the beam that is diffracted by the Au grating which is subsequently reflected from the coherent phonon wavepacket and the other one is the beam that is reflected from the surface of the sample.

In order to validate our explanation, we analyze the intensity of the acoustic interferometry signal as a function of the probe wavelength and the incidence angle. For that purpose, we are interested in the interaction of  $p$ -polarized light that has been transmitted through the Au grating with coherent phonons in the far-field region. Hence, we analyze the acousto-optical coupling at times  $t < -50$  ps, when the coherent wavepacket has not yet reached the BiIG layer but is propagating through the GGG substrate. The phonons modulate components of the dielectric permittivity  $\delta\epsilon_{xx} = \delta\epsilon_{yy} = -\epsilon^2 p_{12} u_{zz}(z, t)$  and  $\delta\epsilon_{zz} = -\epsilon^2 p_{11} u_{zz}(z, t)$ , which are affected by the strain  $u_{zz}(z, t)$  caused by the acoustic wavepacket where the  $p_{ij}$  are the photoelastic parameters. The strain-induced perturbation can be analyzed using perturbative solutions of the Maxwell equations.<sup>23</sup> For the period of our grating structure ( $d$ ) and the experimental conditions ( $\lambda$  and  $\alpha$ ), only non-diffracted light and light of the first negative diffraction order can penetrate into the GGG substrate, while in air only non-diffracted light exists in the far-field zone. Therefore, we obtain the following expression for the relative change of reflectivity,  $\delta R/R$  ( $R$  being the stationary reflectivity without strain pulse)

$$\begin{aligned} \frac{\delta R}{R} = & \sqrt{2\pi} \epsilon Re \left( \frac{1}{ik_0 r_{00}^{(+)}} t_{00}^{(-)} t_{00}^{(+)} f_{\omega_0} (p_{11} k_{\parallel}^2 - p_{12} k_0^2) \exp(-i\omega_0 t) \right. \\ & \left. + \frac{1}{ik_{-1} r_{00}^{(+)}} t_{-10}^{(-)} t_{-10}^{(+)} f_{\omega_{-1}} \left( p_{11} \left( k_{\parallel} - \frac{2\pi}{d} \right)^2 - p_{12} k_{-1}^2 \right) \exp(-i\omega_{-1} t) \right). \end{aligned} \quad (3)$$

Here  $k_{\parallel} = k \sin \alpha$ ,  $k_0 = \sqrt{k^2 \epsilon - k_{\parallel}^2}$ , and  $k_{-1} = \sqrt{k^2 \epsilon - (k_{\parallel} - 2\pi/d)^2}$ , where  $k$  is the photon wavenumber in vacuum, and  $r_{00}^{(+)} (t_{mn}^{+,-})$  are the complex coefficients of the reflection (transmission) amplitudes for the magnetic light component in the periodic structure without strain, respectively. The upper index in  $t_{mn}^{(+,-)}$  indicates light incident from the air (+) or GGG (-) side. The lower indexes in  $t_{mn}^{+,-}$  indicate the diffraction order of the incident ( $m$ ) and transmitted ( $n$ ) light. The first term in Eq. (3) describes Brillouin oscillations with frequency  $\omega_0$  due to non-diffracted light scattered by coherent phonons ( $m = n = 0$ ). The second term in Eq. (3) describes oscillations with frequency  $\omega_{-1}$  due to the scattering of diffracted light of the first negative order. Equation (3) takes into account that for  $t < 0$  the strain fulfills the condition  $u_{zz}(z, t) = f(t - z/s)$  with the Fourier components  $f_{\omega} = \frac{1}{\sqrt{2\pi}} \int_{-\infty}^{+\infty} f(\tau) \exp(i\omega\tau) d\tau$ . The explicit determination of the reflection- and transmission-coefficients and their calculation are given in the supplementary material.<sup>23</sup>

Equation (3) can be used to estimate the amplitudes of the oscillations in the probe signal  $\Delta I_{p-s}(t)$  at frequencies  $\omega_0$  and  $\omega_{-1}$ . The calculated dependences of  $t_{mn}^{+,-}$  on the optical wavelength  $\lambda$  are shown in Fig. 3 for non-diffracted (a) and diffracted (b) light for an incidence angle  $\alpha = 7^\circ$ . The Brillouin oscillations have a sufficient amplitude only if the grating is transparent for light, which means that the factors  $t_{00}^{(-)} t_{00}^{(+)} / r_{00}^{(+)}$  and  $t_{-10}^{(-)} t_{-10}^{(+)} / r_{00}^{(+)}$  should be non-negligible. To that end, the BiIG layer which possesses a waveguiding mode expands the spectral region where these fractions are not negligible and thus the light may penetrate through the Au grating into GGG and back from GGG to air. This explains the fact that the oscillations at  $t < 0$  have not been observed in the samples without the BiIG layer, because at  $\lambda = 800$  nm and reliable values of  $\alpha$  in these samples  $r_{00}^{(+)} \approx 1$ .<sup>14</sup>

The oscillations with  $\omega_{-1}$  due to the diffracted light may be observed only for  $\alpha > \alpha_c$ , where  $\alpha_c$  is a critical angle below which the light diffracted by the Au grating does not propagate inside GGG. The dependence of  $\alpha_c$  on the probe

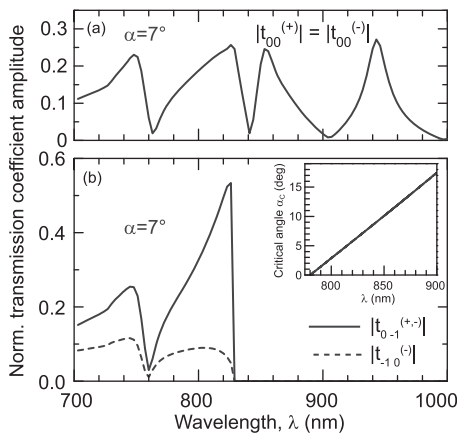


FIG. 3. Calculated amplitude transmission spectra of the magnetic field component of  $p$ -polarized light for non-diffracted (a) and first negative order diffracted (b) light. The inset in (b) shows the dependence of the critical angle  $\alpha_c$  on wavelength  $\lambda$ .

wavelength  $\lambda$  is shown in the inset of Fig. 3(b). The oscillation amplitude also depends on the efficiency of the acousto-optical coupling. In particular, a considerable enhancement of the modulation at  $\omega_{-1}$  is expected for incidence angles at which the diffracted wave in the GGG layer is close to the angle of total internal reflection where  $k_{-1}$  is very small. In this case, the probe beam inside GGG is incident on the acoustic wavepacket front under a large oblique angle (for  $\alpha = 7^\circ$ , this angle equals to  $76^\circ$ ). Thus, the path of the diffracted light through the region with coherent phonons is considerably longer in comparison to the non-diffracted component which is propagating almost perpendicular to the front of the acoustic wavepacket. Finally, the oscillation amplitude obviously depends on the spectral density  $f_\omega$  of the coherent phonons.

Taking the ratio of photo-elastic coefficients  $p_{11}/p_{12} \approx 3$ ,<sup>21</sup> typical strain pulse parameters,<sup>20</sup> and phonon attenuation in GGG,<sup>24</sup> we estimate the spectral amplitudes  $f_\omega$  for  $\omega_0$  and  $\omega_{-1}$  to be close to each other. From Eq. (3) for  $\alpha = 7^\circ$  and  $\lambda = 800$  nm, we then find that the amplitude at  $\omega_{-1}$  is about 12 times larger than at  $\omega_0$ . Such a big difference explains the small intensity of the  $\omega_0$  component in the measured signal  $\Delta I_{p-s}(t)$ . The oscillations at  $t < 0$  are not observed at  $\alpha = 2^\circ$  and  $\alpha = 24^\circ$ , in agreement with theory. Indeed, for  $\lambda = 800$  nm, the incident angle  $\alpha = 2^\circ$  is smaller than the critical angle  $\alpha_c$  and the diffracted component in GGG is absent. For  $\alpha = 24^\circ$ , the value of  $\lambda = 800$  nm is far from the optical resonances and consequently  $t_{00}^{(-)}/t_{00}^{(+)} \approx 0$ , which means that for this incidence angle the far-field probing with coherent phonons in GGG has very low efficiency.

The main reason for the decay of the observed oscillations with increasing negative delay at  $t < 0$  is the finite spectral width of the optical probe pulse. Each spectral component of the pulse gives rise to oscillations at slightly different frequency, which is registered as a decay of the oscillations. The corresponding decay time can be estimated as  $c_0\tau(d\omega_{-1}/dk)^{-1}$ , where  $\tau = 150$  fs is the duration of the optical probe pulse and  $c_0$  is the speed of light. This estimation provides a decay time of about 400 ps, which is close to the experimental observation.

In summary, we have observed a picosecond acoustic interferometric signal (i.e., Brillouin oscillations), which results from the interaction of light diffracted into the studied sample by a periodic grating with GHz coherent phonons. The signal is observed in the temporal interval before the phonons reach the interface with the grating. The amplitude of the observed Brillouin oscillation corresponding to the diffracted light is dominant in the experimentally measured signal. The results agree with the theoretical calculations which provide equations for estimating the oscillation amplitudes for zero and first order diffracted light.

Probing of the internal optical far-field with coherent phonons in samples with periodic structures provides an instrument for measuring the electromagnetic field inside the sample. It is important to note that the acoustic interferometric signal is governed by the angular distribution of light inside the sample and thus reflects the interaction of light excitations in the periodic structures (plasmon-polaritons and waveguiding modes in our particular case). Standard optical techniques, established for probing the optical far-field outside the sample, cannot be easily applied for internal probing. Measuring the spatial far-field distribution of light diffracted by the planar periodic nanostructure shows its potential in acoustic nanoscopy.<sup>17</sup> For instance, the Fourier image of the nanostructure may be obtained by analyzing the spectrum of the acoustic interferometric signal. The grating is the simplest example which shows the reliability of the method and a possibility of applying it to sophisticated planar nanostructures, like two-dimensional photonic crystals.

We acknowledge the support by the Deutsche Forschungsgemeinschaft (DFG 1549/14-1). V.I.B. acknowledges fundings by the Russian Foundation for Basic Research (Nos. 12-02-33100 and 11-02-00681) and the Russian Federal Targeted Program.

<sup>1</sup>H. N. Lin, R. J. Stoner, H. J. Maris, and J. Tauc, *J. Appl. Phys.* **69**, 3816 (1991).

<sup>2</sup>O. B. Wright, *J. Appl. Phys.* **71**, 1617 (1992).

<sup>3</sup>R. Cote and A. Devos, *Rev. Sci. Instrum.* **76**, 053906 (2005).

<sup>4</sup>O. B. Wright, B. Perrin, O. Matsuda, and V. E. Gusev, *Phys. Rev. B* **64**, 081202 (2001).

<sup>5</sup>P. Babilotte, P. Ruello, D. Mounier, T. Pezeril, G. Vaudel, M. Edely, J.-M. Breteau, V. Gusev, and K. Blary, *Phys. Rev. B* **81**, 245207 (2010).

<sup>6</sup>F. Yang, T. J. Grimsley, S. Che, G. A. Antonelli, H. J. Maris, and A. V. Nurmikko, *J. Appl. Phys.* **107**, 103537 (2010).

<sup>7</sup>E. Pontecorvo, M. Ortolani, D. Polli, M. Ferretti, G. Ruoocco, G. Cerullo, and T. Scopigno, *Appl. Phys. Lett.* **98**, 011901 (2011).

<sup>8</sup>R. Liu, G. D. Sanders, C. J. Stanton, C. S. Kim, J. S. Yahng, Y. D. Jho, K. J. Yee, E. Oh, and D. S. Kim, *Phys. Rev. B* **72**, 195335 (2005).

<sup>9</sup>A. V. Akimov, Y. Tanaka, A. B. Pevtsov, S. F. Kaplan, V. G. Golubev, S. Tamura, D. R. Yakovlev, and M. Bayer, *Phys. Rev. Lett.* **101**, 033902 (2008).

<sup>10</sup>A. S. Salasyuk, A. V. Scherbakov, D. R. Yakovlev, A. V. Akimov, A. A. Kaplyanskiy, S. F. Kaplan, S. A. Grudinkin, A. V. Nashchekin, A. B. Pevtsov, V. G. Golubev, T. Berstermann, C. Brüggemann, M. Bombeck, and M. Bayer, *Nano Lett.* **10**, 1319 (2010).

<sup>11</sup>L. L. Guyader, A. Kirilyuk, T. Rasing, G. A. Wurtz, A. V. Zayats, P. F. A. Alkemade, and I. I. Smolyaninov, *J. Phys. D: Appl. Phys.* **41**, 195102 (2008).

<sup>12</sup>G. A. Antonelli, H. J. Maris, S. G. Mallhotra, and J. M. E. Harper, *J. Appl. Phys.* **91**, 3261 (2002).

<sup>13</sup>S.-C. Yang, H.-P. Chen, H.-H. Hsiao, P.-K. Wei, H.-C. Chang, and C.-K. Sun, *Opt. Express* **20**, 16186 (2012).

<sup>14</sup>C. Brüggemann, A. V. Akimov, B. A. Glavin, V. I. Belotelov, I. A. Akimov, J. Jäger, S. Kasture, A. V. Gopal, A. S. Vengurlekar, D. R. Yakovlev, A. J. Kent, and M. Bayer, *Phys. Rev. B* **86**, 121401 (2012).

<sup>15</sup>P.-A. Mante, H.-Y. Chen, M.-H. Lin, Y.-C. Wen, S. Gwo, and C.-K. Sun, *Appl. Phys. Lett.* **101**, 101903 (2012).

- <sup>16</sup>H.-P. Chen, Y.-C. Wen, Y.-H. Chen, C.-H. Tsai, K.-L. Lee, P.-K. Wei, J.-K. Sheu, and C.-K. Sun, *Appl. Phys. Lett.* **97**, 201102 (2010).
- <sup>17</sup>K.-H. Lin, C.-M. Lai, C.-C. Pan, J.-I. Chyi, J.-W. Shi, S.-Z. Sun, C.-F. Chang, and C.-K. Sun, *Nat. Nanotechnol.* **2**, 704 (2007).
- <sup>18</sup>V. I. Belotelov, I. A. Akimov, M. Pohl, V. A. Kotov, S. Kature, A. S. Vengurlekar, A. V. Gopal, D. R. Yakovlev, A. K. Zvezdin, and M. Bayer, *Nat. Nanotechnol.* **6**, 370 (2011).
- <sup>19</sup>M. Pohl, V. I. Belotelov, I. A. Akimov, S. Kature, A. S. Vengurlekar, A. V. Gopal, A. K. Zvezdin, D. R. Yakovlev, and M. Bayer, *Phys. Rev. B* **85**, 081401 (2012).
- <sup>20</sup>C. Thomsen, H. T. Grahn, H. J. Maris, and J. Tauc, *Phys. Rev. B* **34**, 4129 (1986).
- <sup>21</sup>V. F. Kitaeva, E. V. Zharikov, and I. L. Chisty, *Phys. Status Solidi A* **92**, 475 (1985).
- <sup>22</sup>D. Palik, *Handbook of Optical Constants of Solids* (Academic, San Diego, 1985).
- <sup>23</sup>See supplementary material at <http://dx.doi.org/10.1063/1.4771986> for a detailed theoretical analysis: Theory of acoustic interferometry in plasmonic gratings.
- <sup>24</sup>M. Krzesinska and T. Szuta-Buchacz, *Phys. Status Solidi A* **82**, 421 (1984).